Single- and double-electron transfer in low- and intermediate-energy C^{4+} + He collisions

J. W. Gao,[1,2,*] Y. Wu,[1] N. Sisourat,[2] J. G. Wang,[1] and A. Dubois[2]

[1]*Institute of Applied Physics and Computational Mathematics, 100088 Beijing, China*

[2]*Sorbonne Universités, UPMC Université Paris 06, CNRS, Laboratoire de Chimie Physique–Matière et Rayonnement, 75005 Paris, France*

(Received 4 July 2017; published 13 November 2017)

The electron-capture processes in C^{4+} + He collisions have been studied theoretically using a two-active-electron semiclassical atomic-orbital close-coupling method in a wide energy domain. The results of the present calculations are compared with available theoretical predictions and experimental measurements: very good agreements are found for both total and state-selective single-electron-capture (SEC) and double-electron-capture (DEC) cross sections. We extend the understanding on that system to high energies for which only a single series of data exists. Furthermore, the mechanisms responsible for SEC and DEC processes have been investigated by additional *restricted* two-active-electron and single-active-electron calculations. The role of electronic correlations in the collisions is also discussed.

DOI: 10.1103/PhysRevA.96.052703

I. INTRODUCTION

Electron-capture processes for various carbon ions colliding with atoms or molecules have attracted much attention in the past because of their importance in astrophysics and in the treatment of thermonuclear fusion plasmas. From a fundamental point of view, these systems are also of challenging importance, since their dynamics illustrates the effects of static and dynamical electronic correlations, strong Coulombic interactions, and many-channel close-coupling schemes, especially in the intermediate impact energy domain. In particular, collisions between C^{4+} and He have been extensively studied for several decades up to very recently (see Ref. [1] and references therein). Concentrating on various impact energy (E) domains above eV/u, experimental [2–9] and theoretical [1,5,9–12] investigations have shown that the single-electron-capture (SEC) process

$$C^{4+} + He(1s^2) \rightarrow C^{3+} + He^{+} \tag{1}$$

dominates up to nearly 2 orders of magnitude the double-electron-capture (DEC) process

$$C^{4+} + He(1s^2) \rightarrow C^{2+} + He^{2+} \tag{2}$$

for $E \leqslant 2$ keV/u. Very recently, Yan *et al.* [1] extended these investigations to very low energies, from 6 to 10^{-6} keV/u, using a quantum-mechanical molecular-orbital close-coupling (QMOCC) method. Good agreement with other available measurements and calculations for both total SEC and DEC cross sections have been obtained in the impact energy region where those studies overlapped. However, for energies higher than 3 keV/u, there are still large discrepancies between the available experimental and calculated results as well as a lack of data beyond 10 keV/u. In this energy region the semiclassical atomic-orbital close-coupling (SCAOCC) method is expected to be more appropriate than molecular-orbital (MO)-type approaches and has been applied by Hansen [11] to evaluate total SEC and DEC cross sections for energies up to 11 MeV/u. However, the DEC cross sections obtained by Hansen were found to be smaller than the available experimental measurements, the most likely reason of this discrepancy being the use of restricted-size basis sets, an unavoidable limitation at that time due to the power of the computers.

In the present paper, we study theoretically these two electronic processes in a wide energy region ranging from 0.06 to 300 keV/u. We use a two-active-electron SCAOCC method with large basis sets, ensuring a controlled convergence of the cross sections and providing physical insight on this collision system. Total and state-selective SEC and DEC cross sections are first discussed and compared with available theoretical and experimental results. In a second stage we present additional coupled channel calculations using (i) a one-active-electron basis set, i.e., with no dynamical correlation included, and (ii) two-active-electron basis set restricted to span only SEC channels: comparisons with these two approximations leads to a discussion concerning the role of the electronic correlation during the collision and the underlying mechanisms giving rise to SEC and DEC.

The present paper is organized as follows. In the next section we briefly outline the SCAOCC method used in the present calculations. In Sec. III, we present and discuss the results of total and state-selective SEC and DEC cross sections, followed by a brief conclusion. Atomic units are used throughout, unless explicitly indicated otherwise.

II. THEORY

In the present work, the cross sections of the electronic processes occurring during C^{4+} + He collisions are calculated by a two-active-electron SCAOCC approach which has been previously described, for example, in [15–17]. Here we briefly outline only the main features of the method. The two-electron time-dependent Schrödinger equation (TDSE) is written as

$$\left[H - i\frac{\partial}{\partial t}|_{\vec{r}_1,\vec{r}_2}\right]\Psi(\vec{r}_1,\vec{r}_2,\vec{R}(t)) = 0, \tag{3}$$

where H is the electronic Hamiltonian,

$$H = \sum_{i=1,2}\left[-\frac{1}{2}\nabla_i^2 + V_T(r_i) + V_P\left(r_i^p\right)\right] + \frac{1}{|\vec{r}_1 - \vec{r}_2|}, \tag{4}$$

*junwen.gao@etu.upmc.fr

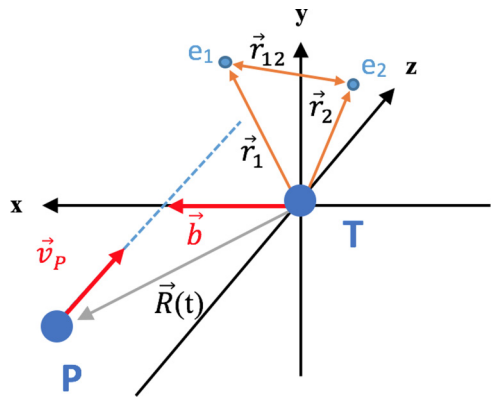

FIG. 1. Collision geometry. The impact parameter $\vec{b}$ and velocity $\vec{v}_P$ define the collision plane (xz) and $\vec{R}(t)$ the projectile (P) trajectory with respect to the target (T). The positions of two electrons with respect to the target center are denoted $\vec{r}_1$, $\vec{r}_2$, and $\vec{r}_{12}$ is the relative vector between the two electrons. Note that for clarity we locate the origin of the reference on the target; this does not restrict the generality of our results, which are Galilean invariant.

and $\vec{r}_i, \vec{r}_i{}^P = \vec{r}_i - \vec{R}(t)$ are the position vectors of the electrons with respect to the target and the projectile, respectively. The relative projectile-target position $\vec{R}(t)$ defines the trajectory, with $\vec{R}(t) = \vec{b} + \vec{v}_P t$ in the usual straight-line, constant velocity approximation where $\vec{b}$ and $\vec{v}_P$ are the impact parameter and velocity, respectively (cf. Fig. 1). The term V_T (V_P) is the electron-target (-projectile) nucleus (and inner electrons, in the frozen-core approximation) potential.

The Schrödinger equation is solved by expanding the wave function onto a basis set composed by states of the isolated collision partners,

$$\begin{aligned}\Psi(\vec{r}_1,\vec{r}_2,\vec{R}(t)) = &\sum_{i=1}^{N_{TT}} c_i^{TT}(t)\Phi_i^{TT}(\vec{r}_1,\vec{r}_2)e^{-iE_i^{TT}t} \\ &+ \sum_{j=1}^{N_{PP}} c_j^{PP}(t)\Phi_j^{PP}(\vec{r}_1,\vec{r}_2,\vec{R}(t))e^{-iE_j^{PP}t} \\ &+ \sum_{k=1}^{N_T}\sum_{l=1}^{N_P} c_{kl}^{TP}(t)\big[\phi_k^T(\vec{r}_1)\phi_l^P(\vec{r}_2,\vec{R}(t)) \\ &\pm \phi_k^T(\vec{r}_2)\phi_l^P(\vec{r}_1,\vec{R}(t))\big]e^{-i(E_k^T+E_l^P)t}, \qquad (5)\end{aligned}$$

where T and TT (P and PP) superscripts denote states and corresponding energies for which one and two electrons are on the target (projectile), respectively. The $+/-$ in the last part of Eq. (5) stands for the singlet/triplet contribution, respectively. For both electrons, the projectile states contain plane-wave electron translation factors (ETFs), $e^{i\vec{v}_P\cdot\vec{r}-i\frac{1}{2}v_P^2 t}$, ensuring Galilean invariance of the results. The insertion of Eqs. (5) into (3) results in a system of first-order coupled differential equations, which can be written in matrix form as

$$i\frac{d}{dt}\mathbf{c}(t) = \mathbf{S}^{-1}(\vec{b},\vec{v},t)\mathbf{M}(\vec{b},\vec{v},t)\mathbf{c}(t), \qquad (6)$$

where $\mathbf{c}(t)$ is the column vector of the time-dependent expansion coefficients, i.e., c^{TT}, c^{PP}, and c^{TP} in Eq. (5), and $\mathbf{S}$, $\mathbf{M}$ are the overlap and coupling matrices, respectively. These equations are solved for a set of initial conditions (initial state i, and given values of b and v) using a robust predictor-corrector time-step method developed by Shampine and Gordon [18]. The probability of a transition $i \to f$ is given by the coefficients c_f ($\equiv c^{TT}$, c^{PP}, or c^{TP}) as

$$P_{fi}(b,v_P) = \lim_{t\to\infty} |c_f(t)|^2. \qquad (7)$$

The corresponding integral (total) cross sections for the considered transition are calculated as

$$\sigma_{fi}(v_P) = 2\pi \int_0^{+\infty} bP_f(b,v_P)db. \qquad (8)$$

For C^{4+}-He collisions, the method presented above is used for the Hamiltonian H, defined in Eq. (4) with

$$V_T(r_i) = -\frac{2}{r_i}, \quad V_P\left(r_i^p\right) = -\frac{4}{r_i^p} - \frac{2}{r_i^p}\left(1+\alpha\, r_i^p\right)e^{-\beta r_i^p}, \qquad (9)$$

where V_T corresponds to He^{2+} and V_P to C^{4+} ion, in the frozen-core electron approximation. The latter is taken from Gargaud *et al.* [13], with the variational parameters $\alpha = 8.360\,572$ and $\beta = 7.726\,25$ optimized in order to reproduce the experimental energy of the C^{3+} levels. In our calculations, a set of 25 Gaussian-type orbitals (GTOs) (13 for $l = 0$, 8 for $l = 1$, and 4 for $l = 2$) are used on the C^{4+} center (16 GTOs, i.e. 10 for $l = 0$ and 6 for $l = 1$, on He^{2+}) and allows the inclusion of 1002 singlet states in total: 146 TT (He), 412 TP (He^+, C^{3+}), and 444 PP (C^{2+}) states. In Table I, we give the energies of the important C^{2+} and C^{3+} states. They are compared with the corresponding experimental data from the NIST tables [14]. The overall agreement between our calculated energies and NIST data is generally very good and at worst equal to about 0.5% for the considered states.

In the same manner as in Ref. [19], the convergence of the results presented in the next section has been checked by computing the cross sections at four distinctive velocities with a series of different GTO basis sets, two of them [20] being larger than that described just above. Comparing the results from these different basis sets, the convergence of both SEC and DEC cross sections was evaluated to be better than 1% in the low impact energy region, to be about 5% for intermediate energies, reaching a maximum of 10% at the highest impact energy ($E = 300$ keV/u), for which, however, the values of the cross sections are lower than 10^{-17} cm^2.

III. RESULTS AND DISCUSSION

A. Total SEC and DEC cross sections

In Fig. 2 we present our total SEC cross sections for C^{4+} + He collisions in the energy region 0.06–300 keV/u. Previous experimental [2,4–8] and theoretical [1,5,10–12] results are also displayed in the figure for comparison. The cross sections show a maximum at around 30 keV/u, following the velocity matching criterion, and a rapid decay for decreasing energies; a shoulder, which may be the signature of a molecular-type mechanism, seems to appear at around 0.1 keV/u, but the general agreement between theoretical and experimental data is rather poor in this energy region, so a firm confirmation

TABLE I. Comparison of energies (in a.u.) of C^{2+} and C^{3+} ions calculated using the model potential [13] with the NIST data [14].

C^{3+}				C^{2+}			
State	E_{GTO}	E_{NIST}	Δ[a]	State	E_{GTO}	E_{NIST}	Δ[a]
$1s^2 2s\ ^2S$	−2.3690	−2.3701	0.04%	$1s^2 2s^2\ ^1S$	−4.1253	−4.1299	0.11%
$1s^2 2p\ ^2P$	−2.0754	−2.0760	0.02%	$1s^2 2s2p\ ^1P$	−3.6549	−3.6636	0.24%
$1s^2 3s\ ^2S$	−0.9909	−0.9902	0.07%	$1s^2 2p^2\ ^1D$	−3.4592	−3.4653	0.17%
$1s^2 3p\ ^2P$	−0.9121	−0.9117	0.04%	$1s^2 2p^2\ ^1S$	−3.2886	−3.2983	0.30%
$1s^2 3d\ ^2D$	−0.8883	−0.8898	0.17%	$1s^2 2s3s\ ^1S$	−3.0019	−3.0037	0.06%
$1s^2 4s\ ^2S$	−0.5417	−0.5414	0.05%	$1s^2 2s3p\ ^1P$	−2.9489	−2.9502	0.04%
$1s^2 4p\ ^2P$	−0.5079	−0.5097	0.34%	$1s^2 2s3d\ ^1D$	−2.8594	−2.8702	0.38%
$1s^2 4d\ ^2D$	−0.4981	−0.5005	0.47%	$1s^2 2p3s\ ^1P$	−2.7164	−2.7174	0.04%
				$1s^2 2p4s\ ^1S$	−2.7074	−2.7096	0.08%
				$1s^2 2p3p\ ^1P$	−2.6728	−2.6732	0.02%
				$1s^2 2s4p\ ^1P$	−2.6569	−2.6610	0.15%

[a] $\Delta = |(E_{GTO} - E_{NIST})/E_{NIST}|$.

concerning such a structure cannot be made. It can be observed that our results merge very reasonably into the measurements of Crandall *et al.* [5], Phaneuf and Crandall [4], Ishii *et al.* [8], Iwai *et al.* [6], and Dijkkamp *et al.* [7] in the respective overlapping energy regions. However, they are slightly higher than the experimental data of Ishii *et al.* for energies below 0.3 keV/u and lower with Zwally's data [2] above 1 keV/u. Comparing with available theoretical results, an excellent agreement is observed between the present results and the atomic-orbital close-coupling (AOCC) results of Hansen [11] and, for energies above 0.3 keV/u, the QMOCC results of Yan *et al.* [1] and those reported in Kimura and Olson [10]. For $E < 1$ keV/u, the semiclassical molecular-orbital close-coupling (SCMOCC) results of Errea *et al.* [12] tend to drop faster than our results and present a minimum at about 0.3 keV/u. However, the latter results do not match the experimental data of Ishii *et al.* and Phaneuf *et al.* in shape and magnitude. For the lowest energies considered in the Fig. 2, our results and Hansen's AOCC results lie above the experimental results of Phaneuf and Crandall, Ishii *et al.*, and MO-based calculations [1,10,12]. Since they stem from equivalent atomic-orbital-based approaches, one could speculate that in this energy region (i) the basis sets used in both works may not be large enough to model the active molecular mechanisms responsible for SEC and (ii) the straight-line trajectory approximation starts to fail. We cannot firmly conclude on that issue, since large discrepancies exist among the available data for the lowest energy considered in the present work. Note, finally, that the molecular-orbital close-coupling (MOCC) results reported in Crandall *et al.* [5] underestimate the SEC cross sections in the whole energy region.

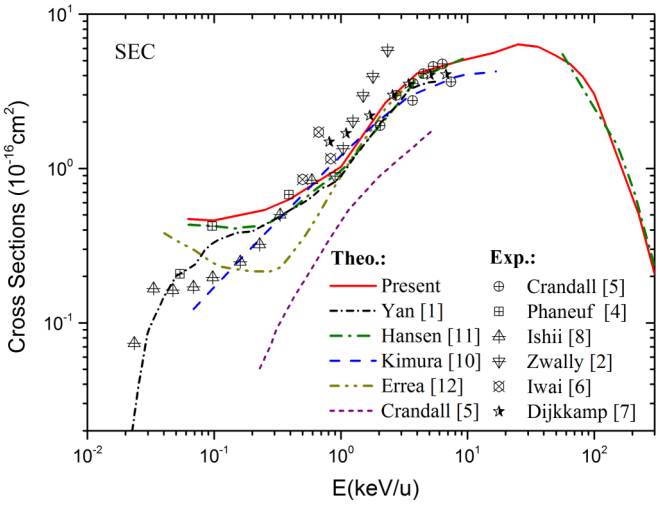

FIG. 2. Single-electron-capture (SEC) cross sections as a function of impact energy. The theoretical results are from the present calculation (red solid line), Yan *et al.* [1] (black short dash-dot line), Hansen [11] (green dash-dot line), Kimura and Olson [10] (blue dash line), Errea *et al.* [12] (dark yellow dash-dot-dot line), Crandall *et al.* [5] (purple short dash line). The experimental results are from Crandall *et al.* [5] (crossed circles), Phaneuf and Crandall [4] (crossed squares), and Ishii *et al.* [8] (crossed up-triangles), Zwally *et al.* [2] (crossed down-triangles), Iwai *et al.* [6] (crossed diamonds), and Dijkkamp *et al.* [7] (stars).

In Fig. 3 the present total DEC cross sections are presented together with the corresponding data stemming from the same work as the ones used for SEC, i.e., [4,5,8] experimental and [1,5,10–12] theoretical investigations. Compared to SEC, the DEC cross sections show a very different behavior as a function of impact energy: a weak dependence from 0.1 to 10 keV/u and a rapid decrease for high and low energies, thus in agreement with the data of Phaneuf and Crandall [4] and Ishii *et al.* [8]. In the intermediate-energy region the present results agree well with the experiments except for $E < 0.1$ keV/u, where our results do not follow the decrease mentioned before. However, comparing with available theoretical calculations, our present results are in excellent agreement with the results of Yan *et al.*, Errea *et al.*, and Crandall *et al.* for $E < 3$ keV/u; note that, in agreement with our data, the QMOCC results of Yan *et al.* and the SCMOCC results of Errea *et al.* do not show the clear decrease observed in [8] for $E < 0.1$ keV/u. This discrepancy may be due to angular scattering effects in the signal collection of the measurement, which tend to underestimate the absolute cross section for very low collision energies [1]. For $E > 3$ keV/u, our results are slightly lower than the QMOCC [1] and SCMOCC [12] results but agree

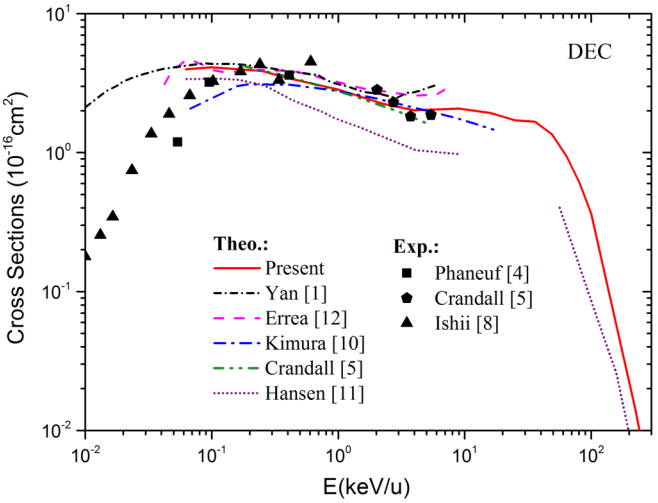

FIG. 3. Comparison between the present DEC cross sections with different experimental and theoretical results as a function of impact energy. The theoretical results are from the present calculation (red solid line), Yan *et al.* [1] (black short dash-dot line), Errea *et al.* [12] (magenta dash line), Kimura and Olson [10] (blue dash-dot line), Crandall *et al.* [5] (green dash-dot-dot line), and Hansen [11] (purple dot line). The experimental results are from Phaneuf and Crandall [4] (solid squares), Crandall *et al.* [5] (solid pentagons), and Ishii *et al.* [8] (solid triangles).

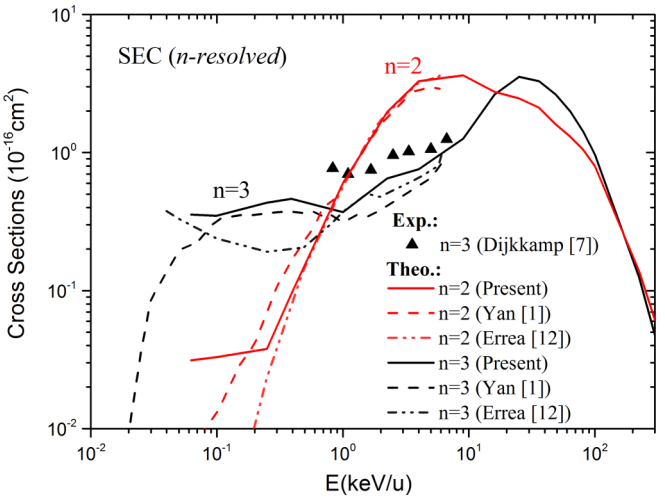

FIG. 4. Comparison between the SEC cross sections for electron capture to the $n = 2$ and 3 shells of the C^{3+} ion with different theoretical and experimental results. The theoretical results are from the present calculation (solid lines), Yan *et al.* [1] (dash lines), and Errea *et al.* [12] (dash-dot-dot lines). The experimental results are from Dijkkamp *et al.* [7] (triangle).

quite well with the experimental results of Crandall *et al.* [5]. It should be noted that an atomic-orbital method is expected to be more appropriate for high impact energies. Moreover, ETFs have not been included in [1] though large in this region. For the entire energy domain considered, the data from Hansen [11] are smaller than most of the theoretical and experimental results. Though stemming from an AOCC approach including ETFs, this failure may be due to the minimal basis set used in these early calculations. Note that for the high energy considered, Hansen's DEC cross sections are also smaller while the SEC ones compare fairly well with ours (see Fig. 2).

B. Shell- and state-selective SEC and DEC cross sections

Figure 4 shows our calculated n-resolved SEC cross sections in comparison with the very few available data [1,7,12]. The analysis is focused on the main capture channels, i.e., $C^{3+}(1s^2 n\ell^1\ ^2L)$ with $n = 2$ and 3. The dominance of the $n = 2$ and $n = 3$ channels follows a complex behavior: our results show that electron capture to the $n = 2$ shell dominates the SEC process in a narrow energy region from 0.8 to 16 keV/u. For this channel, our results are in excellent agreement with the SCMOCC results [12] down to 0.25 keV/u, while the results reported in [1] lie somewhat higher for $E < 1$ keV/u. Note that below 0.25 keV/u, our results show a plateaulike structure which is not confirmed by other results and may illustrate the limitation of our method at low energy (0.06 keV/u). For $n = 3$ electron capture, our results agree slightly better with the measurements of Dijkkamp *et al.* [7] than the other theoretical results. Our results are in good agreement with the results of Yan *et al.* but are larger than the results of Errea *et al.* below 0.8 keV/u energy. This may be due to the absence of $C^{3+}(1s^2 3d^1)$ channels in this latter calculation, explaining the low values of the total SEC cross sections reported in [12] for this energy region (see Fig. 2).

Figure 5 shows our calculated $n\ell$-resolved SEC cross sections together with the data presented in [1,7,12] and from the one-electron SCAOCC approach of Zhao *et al.* [21]. Our results show that electron capture to $C^{3+}(3d)$ is dominant above 20 keV/u. Below this energy electron capture to $C^{3+}(2p)$ takes over until about 0.8 keV/u, for which $C^{3+}(3p)$ starts to dominate. Before commenting on this complex behavior, we will compare our results with the existing data. For electron capture to $C^{3+}(2p)$ [see Fig. 5(a)], our results show a nearly perfect agreement with the only experimental data, that of Dijkkamp *et al.* [7], and the theoretical results [1,12], except for $E < 0.25$ keV/u. The cross sections for capture to $C^{3+}(2s)$ show a similar

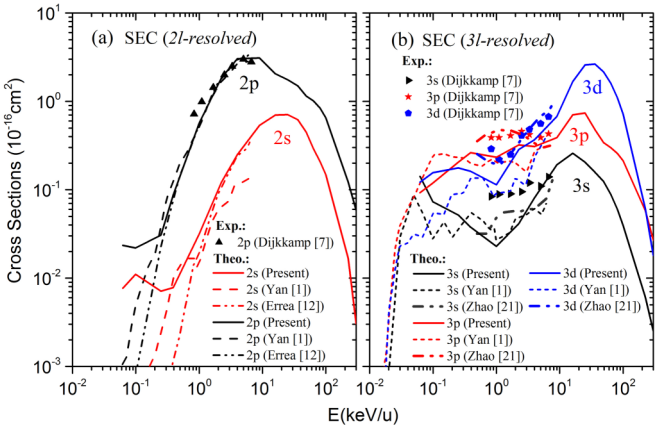

FIG. 5. Comparison between the $n\ell$-selective SEC cross sections as a function of impact energy: (a) for $n = 2$ and (b) for $n = 3$. The data used for comparison are the same as in the previous figures, except for those reported in Zhao *et al.* [21].

behavior, though the agreement with previous theoretical results is less satisfactory; no experimental investigation exists to confirm one or the other series of predictions. The cross sections of Yan *et al.* are slightly smaller than our results for the highest energies, which may be due again to the neglect of the electron translation factors in their calculations. The cross sections shown in Fig. 5(b) correspond for electron capture to $C^{3+}(3\ell)$. The different results are more scattered, though the successive dominance of $3d$ and $3p$ channels agrees with the experimental results [7], which are somewhat higher in magnitude than ours, as the data reported in [21]. In fact, in this energy region, our calculated total SEC cross sections shown in Fig. 2 are also smaller than [7] but are in good agreement with the experimental results of Crandall *et al.* [5], Ishii *et al.* [8], and Iwai *et al.* [6]. For all of the results of the investigations available, the $3s$ channel is the weakest one; for decreasing energies the experimental data decrease more slowly than the theoretical predictions, which present reasonable agreement up to 1 keV/u and with the sudden increase shown in our results. Again, 0.25 keV/u energy may constitute the limit for which the method and the basis set used in the calculations are valid to model some of the weak processes which develop only at low internuclear distances (impact parameters) where refined molecular mechanisms and trajectory effects may take place. Finally, the successive dominance of the $3p$ ($3d$), $2p$, and $3d$ capture channels for increasing energies stems from three different mechanisms which can be illustrated with the energy molecular curves of the CHe^{4+} systems; see Fig. 1 in Errea *et al.* [12] and the note in [22]. For the lowest energies the dominant $3p$ capture proceeds through a complex series of crossings occurring at small internuclear distances (the transition probabilities extend only to impact parameter $b < 2$ a.u.), while for high energies it is a direct atomic mechanism which explains the dominant quasi-resonant $C^{3+}(3d) + He^{+}(1s)$ channels (probabilities fall off only for $b > 7$ a.u.). In between (around 10 keV/u), it is an interplay between a direct mechanism and a molecular one through the avoided crossings at 3.0–3.5 a.u. (cf. Fig. 1 in [12]), which explains the dominance of the $2p$ capture channels. Moreover, the $2p$ and $3p$ cross sections show shoulderlike structures in the energy region above 10 keV/u which also mark the respective decrease and increase of the contributions of the low-b molecular and larger-b direct mechanisms.

State-selective DEC cross sections are presented in Fig. 6, together with the only available theoretical results, those of Yan *et al.* [1] and Errea *et al.* [12]. It can be observed that electron capture to the $C^{2+}(2s^2\ {}^1S)$ state is dominant in the energy region below 20 keV/u, while capture to $C^{2+}(2p^2)$ states takes over for higher energies. It should be noted that the cross section for this latter electronic configuration is totally dominated (>90%) by the contribution of the lowest energy term, i.e., ${}^1D$. For electron capture to the $2s^2$ state, our results agree very well with the QMOCC results of Yan *et al.* and the SCMOCC results of Errea *et al.* in the whole overlapping energy region. The agreement with [1,12] is less satisfactory for the two other electronic configurations, especially for $2s2p$, for which our results are systematically lower than the two previous series of data which agree quite well with each other. For $E > 3$ keV/u the calculations of Yan *et al.* and Errea *et al.* overestimate the total DEC cross sections of Crandall *et al.* [5]

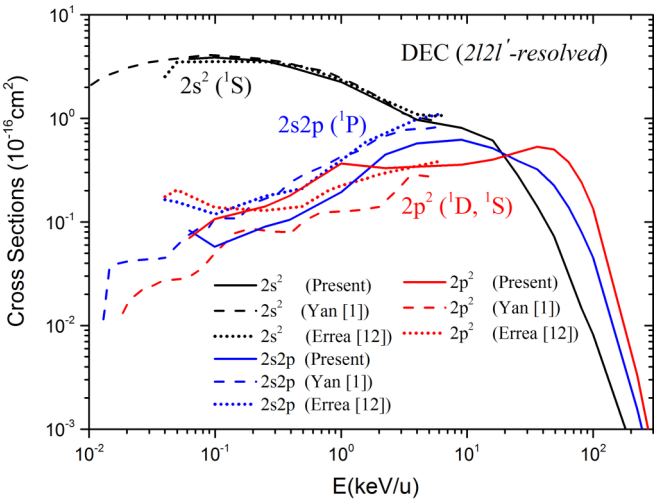

FIG. 6. State-selective DEC cross sections as a function of impact energy. The present calculations are shown by the solid lines, the results of Yan *et al.* [1] by the dash lines, and those of Errea *et al.* [12] by the dot lines.

(see Fig. 3), while our results are in good agreement with these experimental results. Finally, note that for $E = 2$ keV/u our calculations predict an interchange between the contributions of $2s2p$ and $2p^2$ to DEC. This is not observed in the two other calculations where $2s2p$ dominates. This difference may be due to the fact that our large basis set includes the DEC $2sn\ell$ and $2pn\ell$ ($n \geqslant 4$) channels, which may change the dynamics of the collision.

C. Mechanisms for SEC and DEC processes

In order to get further insight to the dynamics of the collision, additional model calculations have been performed: cross sections stemming from two-active-electron calculations with only SEC channels included in the basis set and single-active-electron calculations (using the model potential reported in [17] for He) are shown in Fig. 7. They are compared with the results from our full two-active-electron calculations and from limited-basis (including only SEC channels) calculations of Hansen [11]. The SEC results from single-active-electron calculations are shown to be much larger than the results from our full calculations up to $E < 25$ keV/u impact energy, beyond which both models converge. This tends to prove that electronic correlations play an important role in C^{4+} + He collisions in the low impact energy region. Moreover, using one-electron results total DEC cross sections were also calculated within the independent event model (IEV) and independent particle model (IPM) approximations [23]. In the low impact energy region the results (not shown) from IEV and IPM were found to be much smaller than our full calculations and other theoretical predictions [1,5,10–12], as well as experimental measurements [2,4–8]. This further demonstrates the inadequacy of one-electron models to describe the main electronic processes in C^{4+} + He collisions and the importance of the interelectronic interaction. Comparing the results from our full calculations with the two-electron close-coupling calculations restricted to SEC channels, the good agreement observed in the whole energy region indicates that the SEC

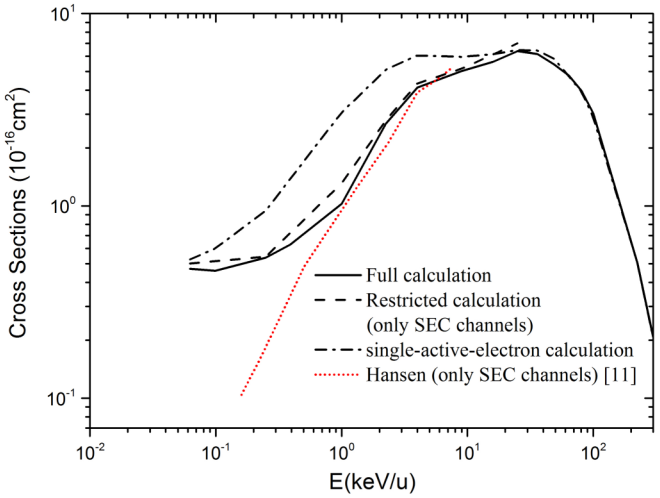

FIG. 7. SEC cross sections as a function of impact energy. Present full calculations: red solid line; two-active-electron calculations with restricted basis set: blue dash line; single-active-electron calculations: black dash-dot line. The results from Hansen [11] are shown with red dotted line.

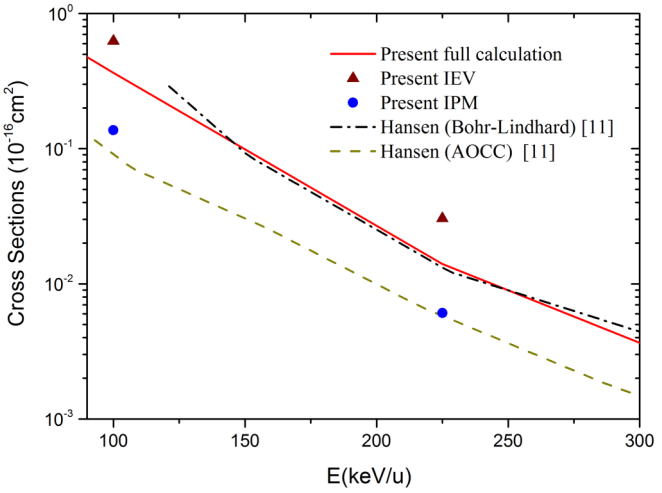

FIG. 9. The DEC cross sections from the present full calculations (red solid line), the present IPM and IEV calculations (solid circles and solid triangles, respectively), SCAOCC calculations (green dashed line), and the Bohr-Lindhard model calculations (black dash-dot line) of Hansen [11].

processes develop independently of the main DEC process. This finding is opposite to Hansen's conclusion stating that SEC is mediated via DEC channels [11] and is drawn in view of the fast decay of the SEC cross sections from his restricted (no DEC channels included) calculations. This behavior does not agree with our equivalent calculations (dashed line in Fig. 7) below $E \approx 1$ keV/u and is certainly due to the very limited basis set used in [11]. To reinforce this conclusion, we present in Fig. 8 the transition probabilities to the main SEC channels $[C^{3+}(1s^2 2p^1)]$ at $E = 0.75$ keV/u collision energy. It was shown in Errea *et al.* [12] (text and Fig. 1) that at low energies this channel is populated through avoided crossings at around 3–4 a.u. internuclear distances. This region implies the $7^1\Sigma$, $2^1\Sigma$, and $3^1\Sigma$ molecular states correlated asymptotically to

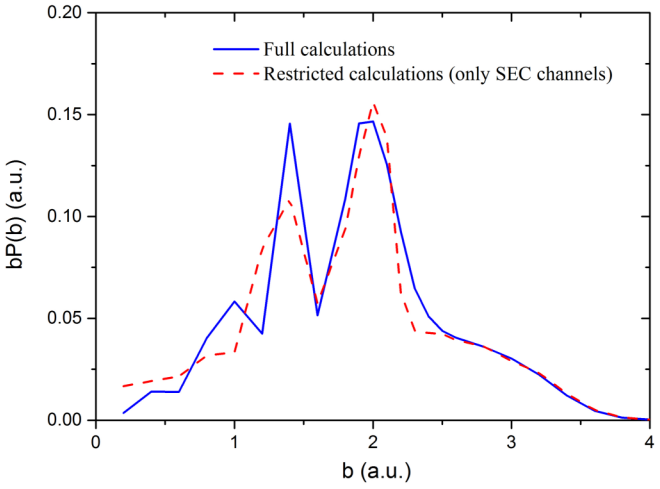

FIG. 8. Transition probabilities for SEC as a function of impact parameter b, for $E = 0.75$ keV/u. The results are from our full calculations (blue solid line) and two-active-electron calculations restricted to SEC channels (red dash line).

the initial $[He(1s^2)]$, SEC $C^{3+}(1s^2 2p^1)$, and DEC $C^{2+}(1s^2 2s^2)$ atomic states. Our results in Fig. 8 show that the probabilities calculated with or without DEC channels (i.e., including or not $3^1\Sigma$) agree with each other in shape and extension, except for only slight differences. This indicates that the reaction takes place directly from $7^1\Sigma$ $[He(1s^2)]$ to $2^1\Sigma$ $[C^{3+}(2p)]$ (in other words, through the radial coupling between these two states, see [24]), without having much interaction with the $3^1\Sigma$ state, as discussed in [12]. This supports the conclusion concerning the weak dependence of SEC dynamics upon DEC processes in the energy domain considered. This is rather in qualitative agreement with previous investigations [3,12,25] that have shown that the DEC processes take place through simultaneous exchange of both electrons in the low impact energy region.

On the contrary, in the high-energy region, Hansen's comparison [11] between SCAOCC calculations and the independent-electron Bohr-Lindhard–type model [26] suggested that the DEC process is dominated by independent-electron-transfer processes. In Fig. 9, these results [11] are compared with our DEC cross sections stemming from full two-electron calculations as well as IEV and IPM approaches. One can observe a surprising agreement between the results of the present full calculations and those stemming from the simple Bohr-Lindhard model. However, though showing similar decays, the results from IEV and IPM are quite different from our close-coupling results. This indicates that electronic correlations are still important in this energy domain, i.e., that the DEC process cannot be described successfully by independent particle processes. In the high impact energy region, the direct two-electron transfer mechanism—from initial state to final state—does dominate also the dynamics of DEC processes. The agreement with the Bohr-Lindhard–type independent-electron predictions reported in [11] may then be simply fortuitous and only restricted to a limited energy domain.

IV. CONCLUSION

In this paper, one- and two-electron processes occurring in the course of C^{4+} + He collisions have been investigated by using the two-active-electron SCAOCC method. Total and state-selective SEC and DEC cross sections have been calculated in a wide energy region 0.06–300 keV/u using a very large basis set to reach controlled reasonable convergence. Our present calculations agree well with available measurements and calculations for both total and state-selective SEC and DEC cross sections in the respective overlapping energy regions. It extends the predictions to high energies, especially for $E > 3$ keV/u, where our present calculations are in better agreement with the experimental data of [5] than the molecular basis set calculations [1,12]. Furthermore, through restricted close-coupling calculations, it is found that electronic correlations play an important role for this collision system, for which the IPM and IEV approximations are found to be in poor agreement with our full calculations, as well as various experimental and theoretical results. We have also demonstrated that contrary to what was concluded in previous investigations, the SEC process is independent of the DEC process in the low impact energy region, where the electron-capture process [$He(1s^2) \rightarrow C^{3+}(2p)$] is dominated by a direct mechanism. At high energies where results are scarce, we have shown that a one-step mechanism dominates the DEC dynamics, in disagreement with a previous investigation in which an independent transfer mechanism was invoked. For that energy domain, experimental investigations will be useful to draw definite conclusions and confirm our data.

ACKNOWLEDGMENTS

J.W.G. is supported by a China Scholarship Council (CSC) scholarship within a CSC-SU program. Y.W. acknowledges the supports of the National Key Research and Development Program of China under Grant No. 2017YFA0402300 and the National Natural Science Foundation of China (Grants No. 11474032, No. 11534011, and No. U1530261). This work was partly supported by LABEX Plas@par (France) under Grant No. ANR-11-IDEX-0004-02.

[1] L. L. Yan, Y. Wu, Y. Z. Qu, J. G. Wang, and R. J. Buenker, Phys. Rev. A **88**, 022706 (2013).
[2] H. J. Zwally, D. W. Koopman, and T. D. Wilkerson, Rev. Sci. Instrum. **40**, 1492 (1969).
[3] M. Barat, P. Roncin, L. Guillemot, M. N. Gaboriaud, and H. Laurent, J. Phys. B **23**, 2811 (1990).
[4] R. A. Phaneuf and D. H. Crandall (unpublished data, reported in [14]).
[5] D. H. Crandall, R. E. Olson, E. J. Shipsey, and J. C. Browne, Phys. Rev. Lett. **36**, 858 (1976).
[6] T. Iwai, Y. Kaneko, M. Kimura, N. Kobayashi, S. Ohtani, K. Okuno, S. Takagi, H. Tawara, and S. Tsurubuchi, Phys. Rev. A **26**, 105 (1982).
[7] D. Dijkkamp, D. Ciric, A. de Boer, F. J. De Heer, and E. Vlieg, J. Phys. B **18**, 4763 (1985).
[8] K. Ishii, A. Itoh, and K. Okuno, Phys. Rev. A **70**, 042716 (2004).
[9] M. Hoshino, L. Pichl, Y. Kanai, Y. Nakai, M. Kitajima, M. Kimura, Y. Li, H. P. Liebermann, R. J. Buenker, H. Tanaka, and Y. Yamazaki, Phys. Rev. A **75**, 012716 (2007).
[10] M. Kimura and R. E. Olson, J. Phys. B **17**, L713 (1984).
[11] J. P. Hansen, J. Phys. B **25**, L17 (1992).
[12] L. F. Errea, B. Herrero, L. Méndez, and A. Riera, J. Phys. B **28**, 693 (1995).
[13] M. Gargaud, J. Hanssen, R. McCarroll, and P. Valiron, J. Phys. B **14**, 2259 (1981).
[14] A. Kramida, Yu. Ralchenko, J. Reader, and NIST ASD Team, NIST Atomic Spectra Database (ver. 5.3) online, available at http://physics.nist.gov/asd [2017, March 1], National Institute of Standards and Technology, Gaithersburg, MD (2015).
[15] J. P. Hansen, A. Dubois, and S. E. Nielsen, Phys. Rev. A **45**, 184 (1992).
[16] N. Sisourat, I. Pilskog, and A. Dubois, Phys. Rev. A **84**, 052722 (2011).
[17] G. Labaigt, A. Jorge, C. Illescas, K. Béroff, A. Dubois, B. Pons, and M. Chabot, J. Phys. B **48**, 075201 (2015).
[18] L. Shampine and M. Gordon, *Computer Solution of Ordinary Differential Equations: The Initial Value Problem* (Freeman, San Francisco, CA, 1975).
[19] A. Ibaaz, R. E. Hernandez, A. Dubois, and N. Sisourat, J. Phys. B **49**, 085202 (2016).
[20] The two larger basis sets are composed by 1273 and 1417 states, respectively including 196 He, 517 $He^+ - C^{3+}$, 560 C^{2+} states and 224 He, 554 $He^+ - C^{3+}$, 639 C^{2+} states.
[21] Y. Zhao, L. Liu, P. Xue, J. Wang, H. Tanuma, and R. Janev, J. Phys. Soc. Jpn. **79**, 064301 (2010).
[22] Our basis set accurately reproduces these curves when used in the diagonalization of the molecular (CHe^{4+}) Hamiltonian.
[23] A. L. Ford, L. A. Wehrman, K. A. Hall, and J. F. Reading, J. Phys. B **30**, 2889 (1997).
[24] L. F. Errea, B. Herrero, L. Méndez, and A. Riera, Few-Body Syst. **19**, 31 (1995).
[25] M. Barat and P. Roncin, J. Phys. B **25**, 2205 (1992).
[26] N. Bohr and J. Lindhard, Mat. Fys. Medd. K. Dan. Vidensk. Selsk. **28**(7), 1 (1954).